Coastal Dynamics 2009
Paper No. 116

OBSERVATION OF MORPHOLOGY AND FLOW MOTION AT THE RIVER MOUTH OF TENRYU WITH X-BAND RADAR

Satoshi Takewaka[1], Yu Takahashi[2], Yoshimitsu Tajima[3] and Shinji Sato[4]

Abstract

X-Band radar observation has been conducted to observe morphology, flow and waves at the river mouth of Tenryu River, Japan. This imaging radar captures spatial distributions and temporal variation of water lines of the river channel and coast lines, and wave propagation in the shallow area. Breaching of the sand bar by a storm event and its recovery process, and behavior of the front formed at the river mouth by the river discharge are displayed in the study. The river flows into Enshu Coast which is suffering from severe erosion and enhancement of sediment supply from the catchment is planned to ease the degraded coast. The observation, in this context, aims to offer basic understanding of the behavior of the river mouth in morphological and hydrodynamic aspects.

Key words: X-band radar, river mouth, sand bar breaching, river front, coastal remote sensing

1. Introduction

The river Tenryu flows into Enshu Coast which is suffering from severe erosion and enhancement of sediment supply from the catchment is planned to ease the degraded coast. The study, in this context, aims to offer basic understanding of the behavior of the river mouth in morphological and hydrodynamic aspects.

X-Band radar observation has been conducted to observe morphology, flow and waves at the river mouth of Tenryu River, Shizuoka, Japan. This imaging radar captures spatial distributions and temporal variation of water lines of the river channel and coast lines, and wave propagation in the shallow area.

Sand bar at the river mouth breached due to flooding during the attack of the Typhoon T4 in July, 2007. Time averaged images are analyzed to track the breaching of the sand bar by this storm event and its

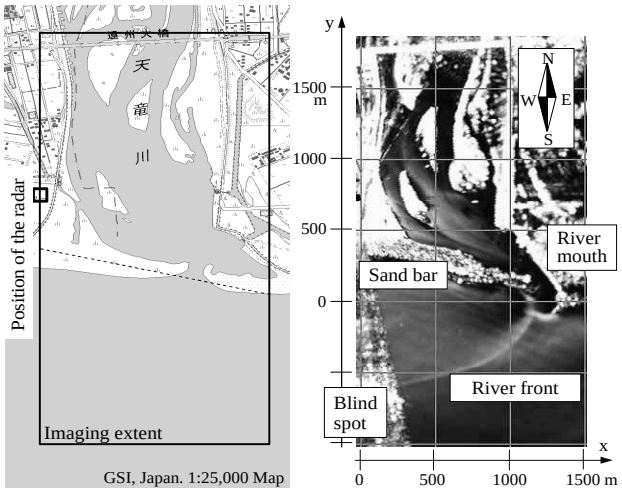

(a) (b)

Figure 1. (a) River mouth of the Tenryu River and location of the radar, and (b) An averaged image (2007 June 8, 21h JST).

[1] Dept. of Eng. System and Energy, University of Tsukuba, Ibaraki 305-8573, Japan. takewaka@kz.tsukuba.ac.jp
[2] ITOCHU Techno-Solutions Corporation.
[3] Dept of Civil Eng., University of Tokyo, Tokyo 113-8656, Japan. yoshitaji@civil.t.u-tokyo.ac.jp
[4] Ditto. sato@civil.t.u-tokyo.ac.jp.

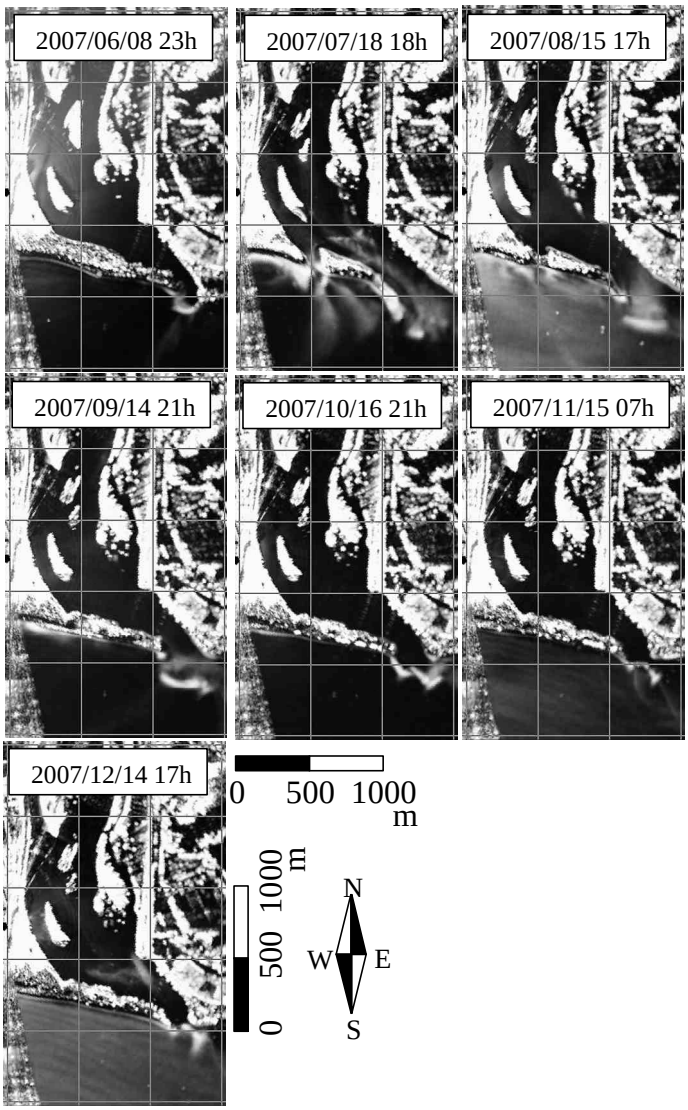

Figure 2. Morphological process of the river mouth. Pre and post situations of sand bar breaching. The images are captured at the same tide level.

recovery process. The width of the main channel increased approximately from 50 m to 250 m. The breached part was buried gradually in the following 18 months and sand bar showed a recovery with supply of sediments from the seaside.

River flow front-like patterns in the vicinity of seaside of the river mouth are observed frequently in the averaged images. The streaky patterns in the averaged images were compared with sea surface colors of a satellite image, confirming river flow front penetration into the coastal water was captured with the radar. Further, a field measurement by towing instruments and statistical analyses on the appearance of the streaks in the radar images are conducted to ensure this speculation.

Depths of the river mouth are estimated from the wave speeds passing the entrance. Response of the water level variations of the river channel and tide with the change of river width is shown.

2. Study Area and X-Band Radar Observation

The radar is installed on the roof of a sewage plant which locates on the right side bank of the river as shown in Figure 1. The measurement started in June 2007 and is still continuing (May, 2009). Two typhoons traveled thorough the vicinity of the area in July and September of 2007. Averaged radar images

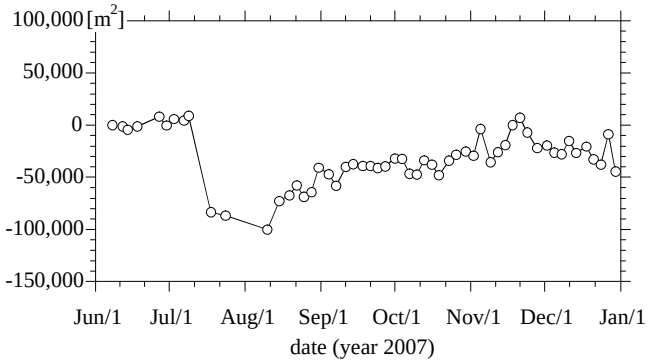

Figure 3. Relative variation of the sand bank area

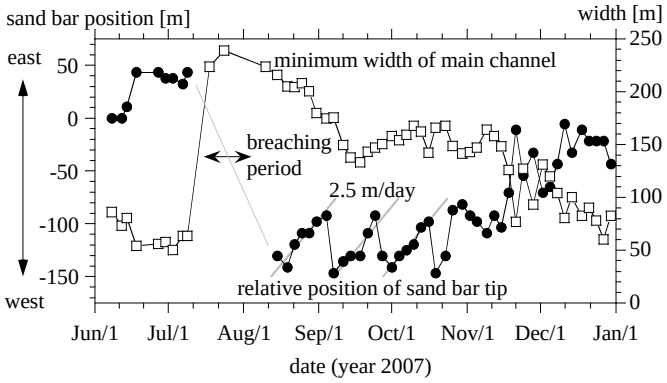

Figure 4. Variation of the relative sand bank tip location and width of the river mouth**.**

over 17 min. are stored hourly and individual radar images are preserved for energetic periods. Features like, water lines of the river channel, shore positions, breaker zone, front formed by the river discharge, etc., are interpreted from the averaged images. Procedures of the radar data analyses for waves and morphology are established in the previous works (Hasan and Takewaka, 2007; Elsayed and Takewaka, 2008).

3. Breaching of the sand bar and its recovery

Typhoon T4 approached the region in the middle of July 2007 accompanied with heavy rainfall, and the flood flow (maximum discharge ~ 9,000 m^3/s) breached the sand bank which was developed at the river mouth. Unfortunately, the radar failed to capture the detailed breaching process due to system trouble; however, amount of the eroded area of the sand bank is estimated from the intermittent averaged images. In the beginning of September 2007, another typhoon T9 traveled along the area and high waves attacked the sand bar, but, deposition was observed rather than erosion this time. The pre/post situations of these storms are shown in Figure 2. Figure 3 and 4 show relative variations of sand bar area, tip location of the sand bar and width of the river mouth, respectively.

Averaged images of Figure 2 indicate that the channel appeared in the sand bar by breaching was almost filled in the following two months, and the widened river mouth narrowed gradually. The image captured in December 2007 shows that the configuration of the area is close to that of the pre-storm situation. Breached amount was approximately 100,000 m^2, and half of this was recovered after 5 months. The recovery of the coastal side of the sand bar was prevailing, suggesting sediment was mainly supplied from the coastal side, which can be also inferred from the eastern migration of the sand bar tip induced by the longshore sediment transport as shown in Figure 4.

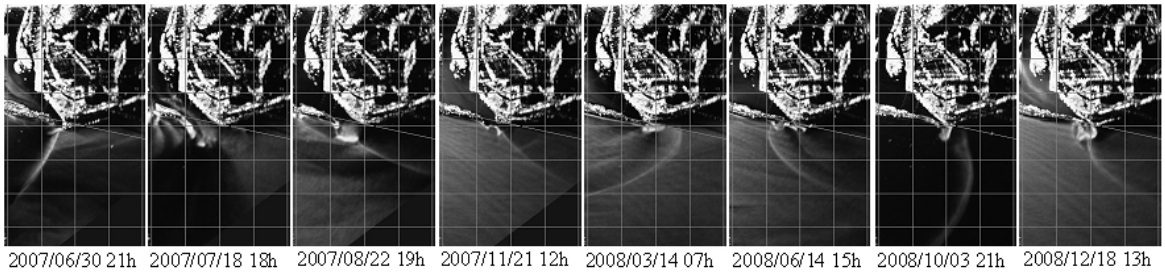

Figure 5. Motion of the river front. The date and time of the observation, tide level and intensity of the river front are attached. Vertical and horizontal lines are drawn for every 500 m.

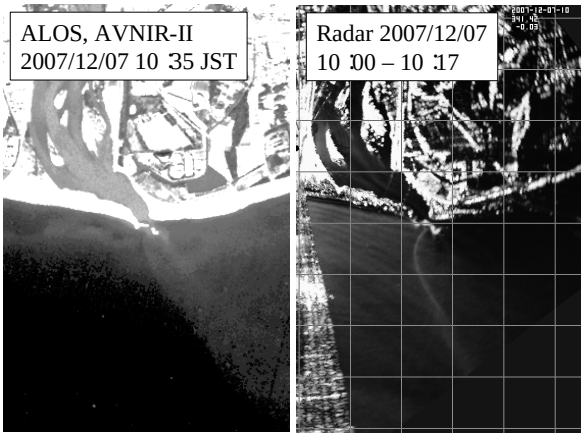

Figure 6. Satellite image (left panel) and averaged radar image (right panel).

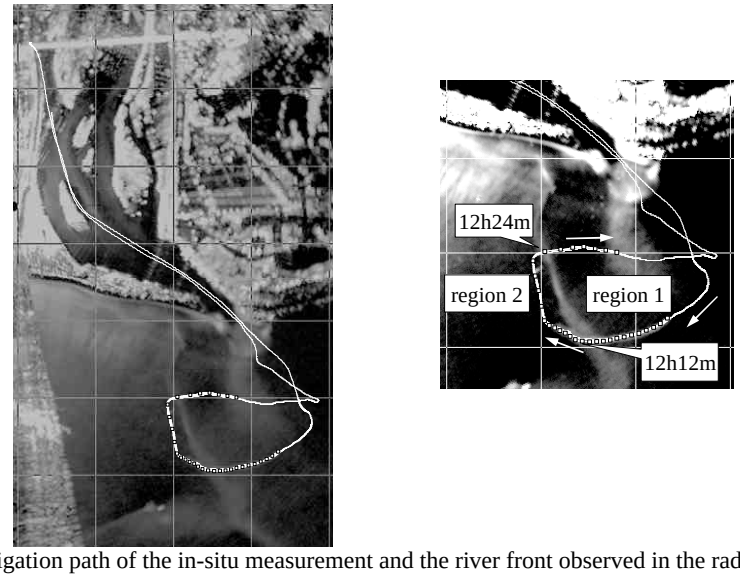

Figure 7. Navigation path of the in-situ measurement and the river front observed in the radar image. 2008 July 24. Left panel: Overall path. Right panel: Close-up of the river front.

4. Motion of the River Water Front

River discharge intrudes into the coastal water and forms a front which is captured in the averaged radar images as shown in Figure 5. It was confirmed that streaky pattern captured in the radar image corresponds

Photo 1. River front observed from the vessel viewing to the NNE. 2008 July 24, 12h11m(JST).

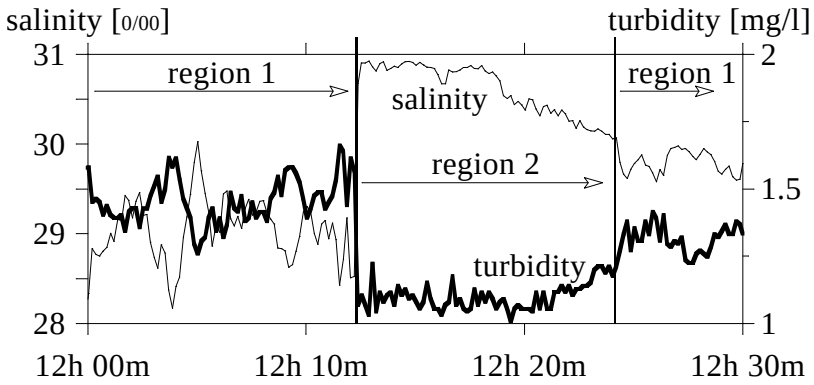

Figure 8. Variation of the salinity and turbidity.

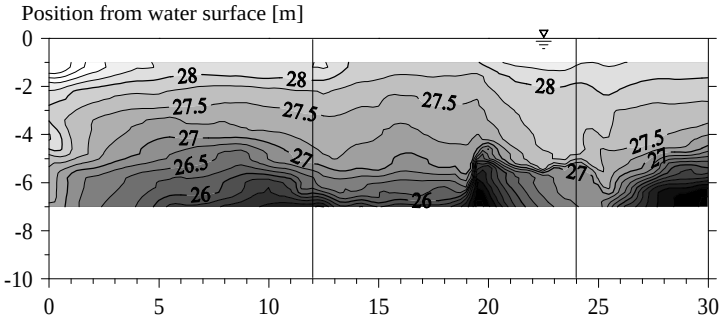

Figure 9. Variation of the vertical water temperature distribution.

to a strip which appeared in satellite remote sensing image where surface color showed a sudden change as shown in Figure 6.

An in-situ towing measurement on water temperature, salinity and turbidity was conducted across the pattern on 2008 July 24th. Figure 7 shows the navigation path with the river front captured in the averaged radar image. The ship crossed the front for two times, approximately at 12 h 12 m and 12 h 24 m. Photo 1 is a snapshot taken from the ship looking into the sand bar at the crossing of the front approximately at 12 h 11 m. Color of the water and growth of wind-ruffled waves showed a sudden jump along the streak. Figure 8 shows the time histories of turbidity and salinity. In region 1, which is the area that should be under the influence of river water, the salinity is relatively low and the turbidity high compared to those measured in region 2. Figure 9 shows the vertical water temperature distribution measured with the thermistor chain. Thermal stratification was formed due to clear sky and solar radiation. When the ship was crossing the

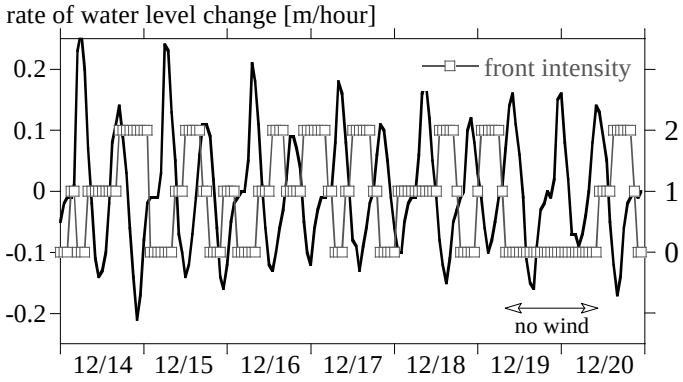

Figure 10. Variation of the speed of the water level change and front intensity.

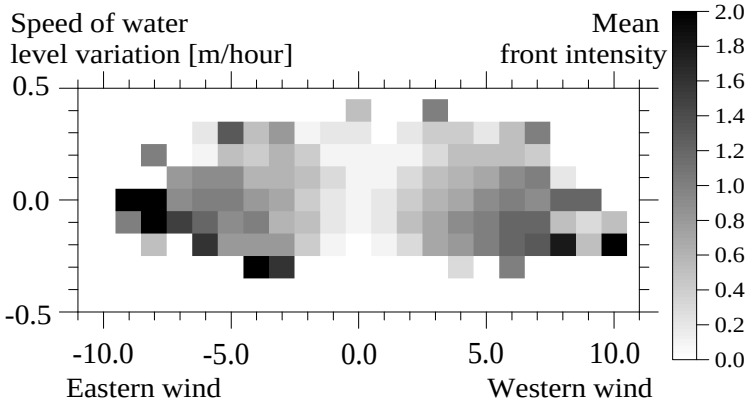

Figure 11. Relationship between front intensity and speed of water level variation and longshore wind component.

front from region 2 to region 1 between 12 h 20 m and 12 h 25m, the stratification was destroyed and water temperature became uniform suggesting f a descending flow was existing there. The results observation is a direct proof that the streaky pattern captured in the averaged radar images corresponds to a river front which is formed by the discharge of fresh water. There must be a converging belt along the front which increases the wave steepness resulting higher return signals in the radar images.

Clearness of the river water front streaks varied in the averaged images. Averaged images for one year from June 2007 have been interpreted to categorize the intensity of the river water front by three levels 0, 1 and 2. Examples of the interpretation are shown in Figure 5. The variation of the intensity with the speed of water level change of the river channel is shown in Figure 10, which shows that the intensities become stronger when the water levels are falling. During these periods, tide is ebbing and river water intrudes in to the sea. There is, however, a period with no front detected in the images even the water level was descending. At these periods, shown in Figure 10, the wind was calm, which suggesting wind breeze plays an important role in detecting river water front. In this context, distributions of the river water front intensities with speed of water level variation and wind speed component along the coastline have been processed, as shown in Figure 11. Higher intensities are frequently observed when the water level is falling and the wind speed exceeds approximately 3 m/s. The river water fronts should be developing even at low wind condition, which are not captured in this study. The radar is capturing ocean waves by emitting electromagnetic waves and detecting echo intensity, which becomes stringer when the directions of emission and wave propagation match. Present layout of the measurement makes difficult to catch the waves which travel normal to the shore.

Averaged images that have two streaks are sometimes captured. This is suggesting that the river flow intrudes into the sea like a jet, however, the detailed analyses remain as a future task. Also the amount and spatial extents of sediments transported by the river flow need clarification.

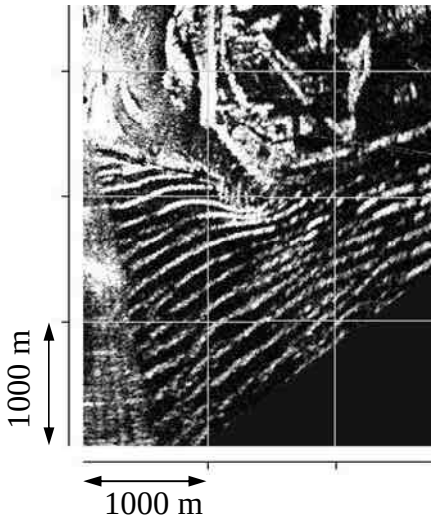

Figure 12. Radar image during high wave period. 2007 September 5 17h JST. Oblique incident waves are observed travelling from the south east.

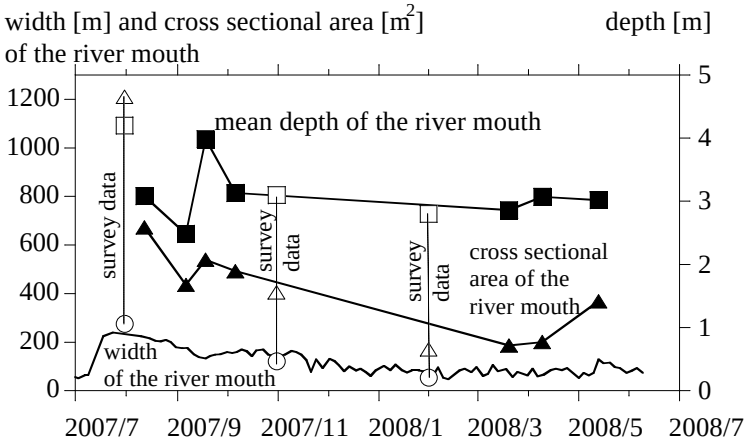

Figure 13. Estimated depth (¦) and cross sectional area (?) of the river mouth. Open symbols indicate survey results.

5. Estimation of the depths of the river mouth

Depths of the river mouth at different periods have been estimated from the speeds of the waves, which travel through the river mouth from ocean side into river channel. Figure 12 is a raw radar image which shows long crested waves approaching the river mouth. The waves travel into the river thorough the entrance on opposing or following current, which is induced by the river discharge and tidal variation.

The speeds of the waves at the river mouth were estimated from the original radar images by analyzing the pixel intensity variation along the entrance. Water depth h of the river mouth was estimated by assuming that waves travel with the speed of a linear long wave and are affected by the current induced from river discharge and tidal variation. Residual R_i at time i is defined as follows:

$$R_i = C_{Ri} - \left(\sqrt{g(h+h_{Oi})} - (-A\frac{dh_{Ri}}{dt} + Q_i)\frac{1}{B(h+h_{Oi})} \right) \quad (1)$$

where, C_{Ri} is the wave speed at the river mouth estimated from the radar images at time i, h is the depth of the river mouth, g is the acceleration due to gravity, $?_{Oi}$ is the ocean water surface elevation, $?_{Ri}$ is the water surface elevation of the river channel, Q_i is the discharge of the river, B is the width of the river mouth estimated from the radar measurement and A is surface area of estuarine basin. Water depth h was estimated to minimize the sum of R_i^2 for a period that the bathymetry is almost unfirm, i.e., h, A and B, can

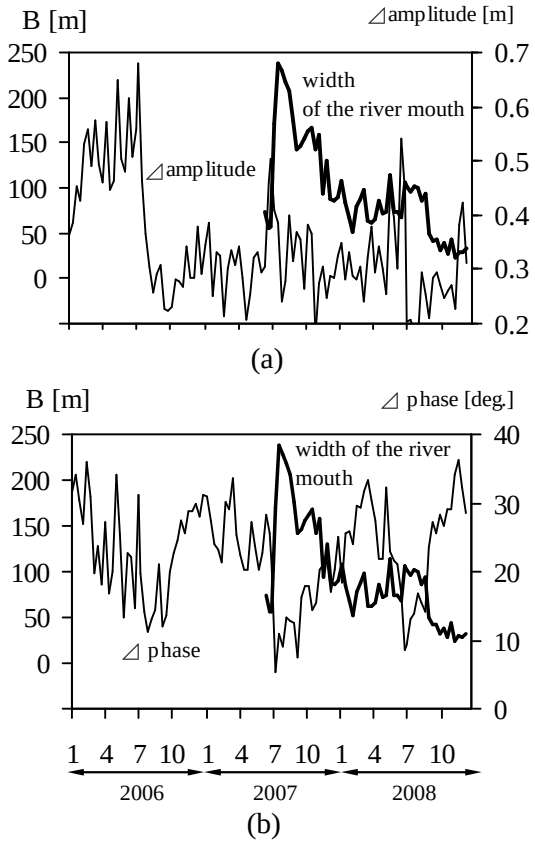

Figure 14. Variations of the (a) amplitude difference and (b) phase difference M_2 components of the ocean tide and river water levels, and width of the river mouth.

be regarded unchanged.

Figure 13 shows the result of the estimation, which displays the variation of water depth *h*, cross sectional area of the river mouth *Bh*. The number of the estimations is restricted, since periods that have sufficient images which captured clearly the wave propagation were just available for high wave conditions (wave height > 3 m). The estimation tracks the contraction of the river mouth after the sand bar breaching. The flood in May, 2008, with maximum discharge of 581 m^3/s, expanded the river mouth, however, the water depth remained almost unchanged.

6. Response of water levels between river channel and ocean tide

Water level variations of the river channel $?_R$ and ocean tide $?_O$ have been analyzed with Fast Fourier Transform. Water level in the river channel is observed at a station which locates 3 km from the river mouth and in the estuarine basin, and ocean tide level at Omaezaki tide station located approximately 40 km eastern from the river mouth. Data length of the Fourier estimation is 512 hours (approximately 21 days) with one hour intervals, and the analyses were done for the records of 2006 to 2008 with intervals of ten days.

The amplitudes and phases of M_2 component (period 12 h 25 m) have been extracted. The amplitude of the tide always exceeds that of river channel and also the phase of the tide is always proceeding. The differences of amplitude and phase are displayed with the river width in Figure 14. The difference of the phase reduces when the river width widens, whereas the difference of amplitude shows no distinct trend and is rather fluctuating. The phase difference dropped dramatically when the sand bar was breached in July, 2007 by the Typhoon T4, and in May, 2008 due to a small flood. Steep falls in both differences indicate that there has occurred an expansion of the river mouth in July, 2006.

7. Concluding remarks

Followings are the results of the X-band observation at the river mouth of Tenryu, which demonstrate the potential of X-band radar as a coastal remote sensing tool:

(1) Sand bar at the river mouth breached due to flooding during the attack of the Typhoon T4 in July, 2007. Time averaged images have been analyzed to track the breaching of the sand bar by this storm event and its recovery process. The width of the main channel increased approximately from 50 m to 250 m. The breached part was buried gradually in the following 18 months and sand bar showed a recovery with supply of sediments from the seaside.

(2) River flow front-like patterns in the vicinity of seaside of the river mouth are observed frequently in the averaged images. The streaky patterns in the averaged images were compared with sea surface colors of a satellite image, confirming river flow front penetration into the coastal water was captured with the radar. Further, a field measurement by towing instruments and statistical analyses on the appearance of the streaks in the radar images were conducted to confirm the streaks captured in the images.

(3) Depths of the river mouth are estimated from the wave speeds passing the entrance. Response of the water level variations of the river channel and tide with the change of river width is shown.

Acknowledgements

The survey data is provided by the courtesy of Ministry of Land, Infrastructure, Transport and Tourism. This research is supported by the Special Coordination Funds for promoting Science and Technology of Ministry of Education, Culture, Sports, Science and Technology and the River Fund, The Foundation of River & Watershed Environment Management.

References

Hasan, G. M. J. and Takewaka, S., 2007. Observation of a stormy wave filed with X-band radar and its linear aspect, *Coastal Engineering Journal*, 49, 149-171.

Elsayed, M. G. and Takewaka, S., 2008. Longshore migration of shoreline mega-cusps observed with X-band radar, *Coastal Engineering Journal*, 50, 247-276.